

## 磁共振三维动脉自旋标记成像量化脑转移瘤放疗前后海马血流灌注变化

刘瑞<sup>1,2</sup>,巩贯忠<sup>2</sup>,杜珊珊<sup>2</sup>,孟康宁<sup>2</sup>,王若峰<sup>3</sup>,尹勇<sup>2</sup>

1.山东第一医科大学(山东省医学科学院)研究生部,山东济南250000;2.山东省肿瘤防治研究院(山东省肿瘤医院)放射物理技术科,山东济南250117;3.新疆医科大学附属肿瘤医院放疗中心,新疆乌鲁木齐830011

**【摘要】目的:**回顾性分析放疗(RT)前后海马血流灌注(CBF)及体积的变化,探究其与剂量的关系,为脑转移瘤(BMs)患者进行全脑放射治疗(WBRT)后海马反应的动态监测提供可行方法。**方法:**回顾性分析43例BM患者RT前后的两次磁共振(MR)模拟定位图像,包括T<sub>1</sub>加权成像(T<sub>1</sub>WI)和三维动脉自旋标记(3D-ASL)成像。在T<sub>1</sub>WI上手动分割左右侧海马结构并统计海马体积,在3D-ASL图像上获取海马CBF。根据两次MR扫描的时间间隔和海马接受剂量分为时间间隔短[<30 d,平均(19.74±7.15) d]≤1 Gy组、1~30 Gy组和≥30 Gy组;时间间隔长[>3个月,平均(495.50±226.06) d]≤1 Gy组、1~30 Gy组和≥30 Gy组。分析RT后海马CBF和体积的变化规律及剂量-效应关系。**结果:**(1)共入组86个海马测量其CBF与体积变化情况,RT后海马CBF最小值(CBF<sub>min</sub>)、最大值(CBF<sub>max</sub>)、平均值(CBF<sub>mean</sub>)及体积较RT前分别减少8.32%、7.31%、8.09%、4.11%(P<0.05);海马CBF<sub>min</sub>、CBF<sub>max</sub>、CBF<sub>mean</sub>的下降率分别较体积减小率高6.33%、7.01%、8.23%。(2)两次MR模拟定位扫描时间间隔短时,≤1 Gy组与1~30 Gy组海马CBF增加,增加率与海马接受的剂量呈正相关,≥30 Gy组海马CBF下降,除≤1 Gy组与1~30 Gy组外,其余剂量组的海马CBF变化率差异均有统计学意义(P<0.05)。(3)两次MR模拟定位扫描时间间隔长时,3个剂量组的海马CBF与体积均呈下降趋势,下降率与海马接受的剂量呈正相关,除≤1 Gy组与1~30 Gy组外,其余剂量组的海马CBF变化率差异均有统计学意义(P<0.05),3个剂量组海马体积减小率的差异均有统计学意义(P<0.05)。**结论:**BMs患者接受RT后海马的CBF下降较体积减小更加敏感,有明显的时间及剂量依赖性,应该作为BM患者在WBRT后追踪海马RT反应和预测放射性损伤的常规生物指标。

**【关键词】**海马;血流灌注;放射治疗;脑转移瘤;磁共振成像;三维动脉自旋标记

**【中图分类号】**R816

**【文献标志码】**A

**【文章编号】**1005-202X(2025)02-0148-06

## Application of three-dimensional arterial spin labeling MR imaging to quantify changes in hippocampal perfusion before and after radiotherapy for brain metastases

LIU Rui<sup>1,2</sup>, GONG Guanzhong<sup>2</sup>, DU Shanshan<sup>2</sup>, MENG Kangning<sup>2</sup>, WANG Ruozheng<sup>3</sup>, YIN Yong<sup>2</sup>

1. Graduate Department, Shandong First Medical University/Shandong Academy of Medical Sciences, Jinan 250000, China; 2. Department of Radiation Physics, Shandong Cancer Institute/Shandong Cancer Hospital, Jinan 250117, China; 3. Radiotherapy Center, Cancer Hospital of Xinjiang Medical University, Urumqi 830011, China

**Abstract:** Objective To retrospectively analyze the changes in cerebral blood flow (CBF) of hippocampus before and after radiotherapy (RT) and to explore its relationship with dose for providing a feasible approach for dynamically monitoring hippocampal response after whole brain radiation therapy in patients with brain metastases (BMs). Methods A retrospective analysis was conducted on magnetic resonance (MR) images from 43 BM patients before and after RT, including T<sub>1</sub>-weighted imaging (T<sub>1</sub>WI) and three-dimensional arterial spin labeling (3D-ASL) imaging. Manual segmentation of the hippocampal structures was performed on T<sub>1</sub>WI to determine hippocampal volume, while CBF within the hippocampus was derived from 3D-ASL images. Patients were categorized into different groups according to the time interval between two MR scans and the dose received by the

**【收稿日期】**2024-10-12

**【基金项目】**山东省自然科学基金(ZR2023MH297)

**【作者简介】**刘瑞,硕士研究生,研究方向:影像引导下的放射治疗,E-mail: LiuRui732116441@163.com

**【通信作者】**尹勇,博士,研究员,博士生导师,主要从事肿瘤放射物理学、肿瘤精确放疗新技术、医学图像处理辅助精确放疗的研究和临床应用工作,E-mail: yinyongsd@126.com

hippocampus, namely short time interval [ $<30$  d, with an average of  $(19.74\pm7.15)$  d]  $\leqslant 1$  Gy, 1-30 Gy and  $\geqslant 30$  Gy groups; long time interval [ $>3$  months, with an average of  $(495.50\pm226.06)$  d]  $\leqslant 1$  Gy, 1-30 Gy and  $\geqslant 30$  Gy groups. The patterns of changes in hippocampal CBF and volume, as well as the dose-effect relationship following RT were analyzed. **Results** (1) A total of 86 hippocampi were enrolled, showing reductions of 8.32% in minimum CBF ( $CBF_{\text{min}}$ ), 7.31% in maximum CBF ( $CBF_{\text{max}}$ ), 8.09% in mean CBF ( $CBF_{\text{mean}}$ ), and 4.11% in hippocampal volume after RT ( $P<0.05$ ). The decrease rates of  $CBF_{\text{min}}$ ,  $CBF_{\text{max}}$  and  $CBF_{\text{mean}}$  were 6.33%, 7.01% and 8.23% higher than the reduction rate of hippocampal volume, respectively. (2) With a brief interval between two MR simulation localization scans, hippocampal CBF in the groups receiving  $\leqslant 1$  Gy and 1-30 Gy exhibited an increase, with the increase rate positively correlated to the radiation dose absorbed by the hippocampus. Conversely, in the group receiving  $\geqslant 30$  Gy, hippocampal CBF decreased. The variations in the rate of hippocampal CBF change across the dose groups were statistically significant, except when comparing  $\leqslant 1$  Gy and 1-30 Gy groups ( $P<0.05$ ). Additionally, the hippocampal volume in all 3 dose groups experienced a slight increase, with the growth rate also positively correlated to the radiation dose received by the hippocampus; however, these differences were not statistically significant ( $P>0.05$ ). (3) With a long interval between MR simulation localization scans, both hippocampal CBF and volume in all 3 dose groups demonstrated decreasing trends, with the decrease rate positively correlated to the radiation dose received by the hippocampus. Statistically significant differences in the rate of CBF change were noted among the dose groups, except for the comparison between  $\leqslant 1$  Gy and 1-30 Gy groups ( $P<0.05$ ). The reduction rate of hippocampal volume across 3 dose groups was statistically significant ( $P<0.05$ ). **Conclusion** The reduction in hippocampal CBF following RT in BMs patients is more sensitive than the reduction in hippocampal volume, exhibiting a pronounced dependence on both time and radiation dose. Consequently, CBF changes should be employed as a standard bioindicator for monitoring the response to hippocampal RT and predicting radiological injuries after whole brain radiotherapy in BMs patients.

**Keywords:** hippocampus; blood flow perfusion; radiotherapy; brain metastasis; magnetic resonance imaging; three-dimensional arterial spin labeling

## 前言

脑转移瘤(Brain Metastases, BMs)是中枢神经系统常见恶性肿瘤,60%的BMs为多发病灶,因此全脑放疗(Whole Brain Radiotherapy, WBRT)在BMs放疗(Radiotherapy, RT)中发挥不可替代的作用<sup>[1-2]</sup>。然而WBRT后认知功能障碍发生率不断增加为严重影响患者的生活质量,已经成为制约WBRT应用的主要因素。WBRT后认知功能障碍与射线导致的海马结构的变化相关。WBRT后的海马血流灌注(Cerebral Blood Flow, CBF)下降造成的缺血缺氧会加速海马结构的破坏,导致体积缩小。Kim等<sup>[3]</sup>研究表明,高剂量射线可引起脑实质和血管内皮细胞的损耗,进而导致血管损伤、狭窄、血流量下降。海马作为一种对低CBF敏感的结构,CBF下降引起的生物效应更加显著<sup>[4]</sup>。以往研究表明海马体积缩小是神经认知功能障碍发生的重要原因,是阿尔兹海默症(Alzheimer's Disease, AD)的有效预测指标<sup>[5]</sup>。在过去的20多年中,带有海马保护的WBRT技术已经在临床进行推广,但尚未取得统一的疗效,其主要原因在于海马RT反应及损伤缺乏明确的剂量-效应关系及监测指标,单纯依靠体积变化难以精确预测海马损伤。基于磁共振(Magnetic Resonance, MR)三维动脉自旋标记(Three-Dimensional Arterial Spin Labeling, 3D-ASL)获得的CBF,为海马RT反应的生

物学追踪提供可行方法。3D-ASL以水分子作为内源性对比剂,无需注射含钆大分子造影剂,不依赖于血脑屏障破坏程度,可客观反映脑组织CBF水平<sup>[6]</sup>。基于3D-ASL测量CBF在追踪BMs的RT反应、鉴别复发及预测放射性损伤方面具有显著的临床应用潜力<sup>[7-8]</sup>。徐耀等<sup>[9]</sup>研究证实脑血流的下降可以作为AD的重要生物学预测指标,而WBRT后海马CBF变化同样可以从生物功能方面反映海马的微观变化。因此,本研究基于3D-ASL量化WBRT前后海马CBF变化情况,分析海马CBF及体积变化与剂量的关系,为追踪BMs患者WBRT后海马的RT反应提供可行的方法。

## 1 资料与方法

### 1.1 病例资料

回顾性分析2018年10月~2023年8月在山东第一医科大学附属肿瘤医院接受WBRT的BMs患者43例。纳入标准:患者均进行RT前后的两次MR模拟定位扫描,且两次都有3D-ASL影像,两次定位之间患者只接受RT。其中男26例,女17例;年龄36~78岁,平均( $58.5\pm3.0$ )岁;原发肿瘤类型包括肺癌31例,乳腺癌8例,其他类型原发癌4例。该研究由山东第一医科大学附属肿瘤医院伦理委员会批准(SDTHEC.2024003117),所有患者均已签署知情同意书。

## 1.2 方法

**1.2.1 MR模拟定位图像获取** 所有患者在RT前后使用GE 3.0T 超导型MR扫描仪(Discovery 750 W, GE Healthcare, Chicago, IL, USA)进行 $T_1$ 加权成像( $T_1$ -Weighted Imaging,  $T_1$ WI)和3D-ASL扫描。 $T_1$ WI扫描参数:TR=8.5 ms, TE=3.2 ms, 矩阵=256×256, FOV=256 mm×256 mm, 层厚=3 mm, 层间距=0 mm。3D-ASL扫描参数:TR=5 160 ms, TE=11 ms, 矩阵=256×256, FOV=256 mm×256 mm, 层厚=3 mm, 激发次数1次, 标记后延迟=2 025 ms。

**1.2.2 海马剂量及体积的测量** 在Varian Eclipse计划系统上获取患者的RT计划,将MR图像和RT计划导入MIM Maestro(7.17 Cleveland, OH, USA)软件,由一名有多年临床治疗经验的放射肿瘤学专家在 $T_1$ WI图像上勾画海马(左右侧海马分开勾画),后由第2位专家进行审核验证,无误后测量海马体积。将RT计划的RT dose及计算机断层扫描(Computed Tomography, CT)图像与完成海马勾画的 $T_1$ WI图像刚性配准,获得海马接受的剂量。

**1.2.3 分组** 43例患者左右两侧海马接受的剂量有差异,且根据曾善美等<sup>[10]</sup>研究发现敲除小鼠肌醇1,4,5-三磷酸受体2型后,左右侧海马CBF变化差异显著,研究认为左右侧海马CBF独立变化。单独分析86个海马CBF与体积变化,按照两次MR模拟定位时间间隔的长短以及海马接受的剂量分为:时间间隔短的≤1 Gy组(15个海马),1~30 Gy组(15个海马),≥30 Gy组(14个海马);时间间隔长的≤1 Gy组(14个海马),1~30 Gy组(13个海马),≥30 Gy组(15个海马)。其中时间间隔短指RT前后两次MR模拟定位时间间隔小于30 d,平均(19.74±7.15) d。时间间隔长指的是RT前后两次MR模拟定位时间间隔大于3个月,平均(495.50±226.06) d。选择≥30 Gy作为高剂量组是参考Goda等<sup>[11]</sup>研究,建议将左海马平均剂量≤30 Gy作为保护认知功能的剂量限值。

**1.2.4 海马CBF的测量** 在GE AW4.7工作站将3D-ASL图像与 $T_1$ WI图像进行刚性配准,以便于观察海马的轮廓。分别测量3次海马区域CBF的最小值(CBF<sub>min</sub>)、最大值(CBF<sub>max</sub>)、平均值(CBF<sub>mean</sub>),后取3次测量值的平均值,并分别计算不同时间间隔不同剂量组海马CBF平均变化率。实验工作流程图见图1。

## 1.3 统计学方法

采用SPSS(version 20.0, IBM, USA)统计学软件进行分析,计量资料用均数±标准差表示,多组间比较采用Kruskal-Wallis H检验,组间两两比较采用

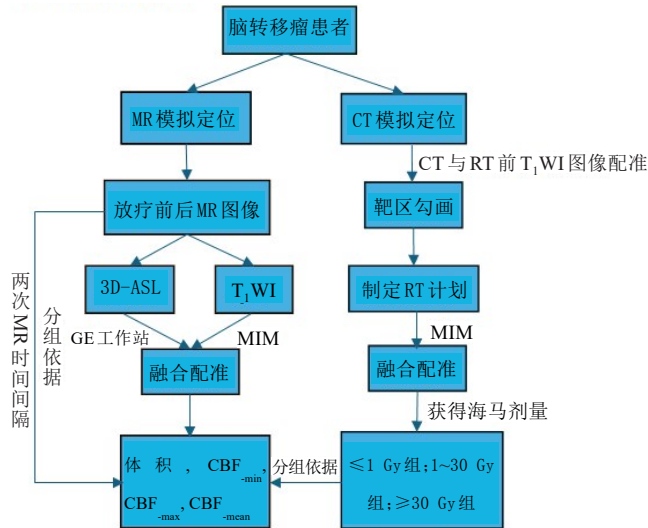


图1 研究流程图

Figure 1 Research flowchart

Dunn检验及Mann-Whitney U检验。 $P<0.05$ 为差异有统计学意义。

## 2 结果

### 2.1 RT前后海马CBF与体积变化分析

共入组86个海马测量其CBF与体积变化情况,测得RT后海马CBF<sub>min</sub>、CBF<sub>max</sub>、CBF<sub>mean</sub>及体积均呈持续下降趋势,较RT前分别平均减少8.32%、7.31%、8.09%、4.11%,差异均有统计学意义( $P<0.05$ );海马CBF<sub>min</sub>、CBF<sub>max</sub>、CBF<sub>mean</sub>的下降率分别较体积减小率高6.33%、7.01%、8.23%。

### 2.2 不同时间间隔剂量分组之间海马CBF及体积变化的分析

**2.2.1 时间间隔短** 两次MR定位时间间隔短组,≤1 Gy组与1~30 Gy组的海马CBF在RT后增加,如图2所示,≥30 Gy组的海马CBF呈下降趋势。RT前后海马CBF与体积如表1所示。3个剂量组海马CBF变化率除≤1 Gy组与1~30 Gy组外,其余组间的差异有统计学意义( $P<0.05$ )。3个剂量组的海马体积略增长,增长率的差异无统计学意义( $P>0.05$ ),体积增长率与海马接受剂量呈正相关。RT前后海马CBF、体积变化率及组间和组内的差异如表2所示。

**2.2.2 时间间隔长** 两次MR定位时间间隔长组,3个剂量组的海马CBF及体积均呈下降趋势,如表1所示,CBF变化如图3所示。海马CBF及体积下降率与海马接受的剂量呈正相关,3个剂量组之间的海马CBF变化率除≤1 Gy组与1~30 Gy组外,其余组间的差异有统计学意义( $P<0.05$ ),体积组间下降率差异均有统计学意义( $P<0.05$ ),如表2所示。

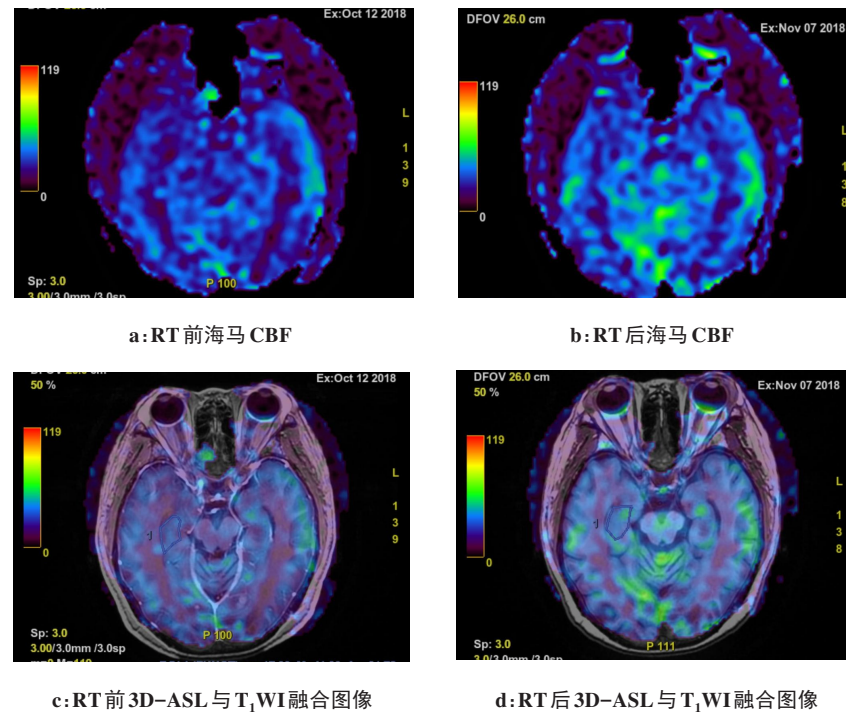


图2 短时间间隔RT前后海马CBF变化

Figure 2 Hippocampal CBF changes at brief intervals before and after radiotherapy

表1 RT前后海马CBF与体积( $\bar{x} \pm s$ )Table 1 Hippocampal CBF and volume before and after radiotherapy (Mean $\pm$ SD)

组别	时间间隔短组/ $\text{mL} \cdot 100 \text{ g}^{-1} \cdot \text{min}^{-1}$			时间间隔长组/ $\text{mL} \cdot 100 \text{ g}^{-1} \cdot \text{min}^{-1}$			时间间隔短组	时间间隔长组	
	CBF <sub>min</sub>	CBF <sub>max</sub>	CBF <sub>mean</sub>	CBF <sub>min</sub>	CBF <sub>max</sub>	CBF <sub>mean</sub>			
$\leq 1 \text{ Gy}$	放疗前	20.48 $\pm$ 7.31	46.02 $\pm$ 15.08	35.88 $\pm$ 12.66	31.33 $\pm$ 5.56	62.41 $\pm$ 8.62	47.78 $\pm$ 4.87	2.89 $\pm$ 0.56	3.56 $\pm$ 0.78
	放疗后	21.09 $\pm$ 7.45*	48.72 $\pm$ 14.38*	38.17 $\pm$ 14.44*	28.00 $\pm$ 5.51*	52.46 $\pm$ 8.88*	41.25 $\pm$ 8.42*	2.90 $\pm$ 0.56	3.21 $\pm$ 0.81*
$1\sim 30 \text{ Gy}$	放疗前	23.48 $\pm$ 3.56	53.11 $\pm$ 8.33	38.36 $\pm$ 5.81	26.07 $\pm$ 5.34	61.70 $\pm$ 6.00	41.72 $\pm$ 7.99	3.25 $\pm$ 0.57	3.45 $\pm$ 0.35
	放疗后	26.14 $\pm$ 3.25*	61.77 $\pm$ 13.49*	43.24 $\pm$ 6.93*	22.35 $\pm$ 5.69*	50.79 $\pm$ 9.05*	34.37 $\pm$ 7.75*	3.26 $\pm$ 0.56	2.95 $\pm$ 0.45*
$\geq 30 \text{ Gy}$	放疗前	27.00 $\pm$ 9.78	57.13 $\pm$ 14.99	44.10 $\pm$ 13.49	34.19 $\pm$ 3.25	74.19 $\pm$ 9.85	53.55 $\pm$ 7.94	3.11 $\pm$ 0.58	3.77 $\pm$ 0.32
	放疗后	22.66 $\pm$ 7.58*	45.85 $\pm$ 11.16*	36.77 $\pm$ 10.32*	27.37 $\pm$ 3.36*	56.12 $\pm$ 5.89*	41.43 $\pm$ 5.83*	3.20 $\pm$ 0.63	3.10 $\pm$ 0.36*

\*表示与放疗前对比,  $P < 0.05$ 表2 RT前后海马CBF与体积变化率(%,  $\bar{x} \pm s$ )Table 2 Rates of change in hippocampal CBF and volume before and after radiotherapy (%), Mean $\pm$ SD

组别	CBF <sub>min</sub>	CBF <sub>max</sub>	CBF <sub>mean</sub>	体积
$\leq 1 \text{ Gy}$ 组	3.10 $\pm$ 2.30	7.78 $\pm$ 12.50	5.66 $\pm$ 5.11	0.15 $\pm$ 0.23
时间间隔短组	1~30 Gy组	12.10 $\pm$ 8.81	16.46 $\pm$ 17.55	13.72 $\pm$ 16.72
$\geq 30 \text{ Gy}$ 组	-15.03 $\pm$ 9.94 <sup>ab</sup>	-19.21 $\pm$ 5.35 <sup>ab</sup>	-16.10 $\pm$ 8.47 <sup>ab</sup>	0.33 $\pm$ 0.01
时间间隔长组	$\leq 1 \text{ Gy}$ 组	-10.82 $\pm$ 8.14 <sup>c</sup>	-15.45 $\pm$ 12.21 <sup>c</sup>	-13.33 $\pm$ 16.47 <sup>c</sup>
$1\sim 30 \text{ Gy}$ 组	-14.82 $\pm$ 9.06 <sup>c</sup>	-17.19 $\pm$ 15.26 <sup>c</sup>	-16.89 $\pm$ 13.37 <sup>c</sup>	-14.59 $\pm$ 1.14 <sup>ac</sup>
$\geq 30 \text{ Gy}$ 组	-19.88 $\pm$ 7.71 <sup>abc</sup>	-23.82 $\pm$ 7.37 <sup>abc</sup>	-22.07 $\pm$ 9.15 <sup>abc</sup>	-17.65 $\pm$ 2.32 <sup>abc</sup>

同组间比较, 与 $\leq 1 \text{ Gy}$ 组比较,<sup>a</sup> $P < 0.05$ , 与 $1\sim 30 \text{ Gy}$ 组比较,<sup>b</sup> $P < 0.05$ ; 与时间间隔短组同剂量组间比较,<sup>c</sup> $P < 0.05$

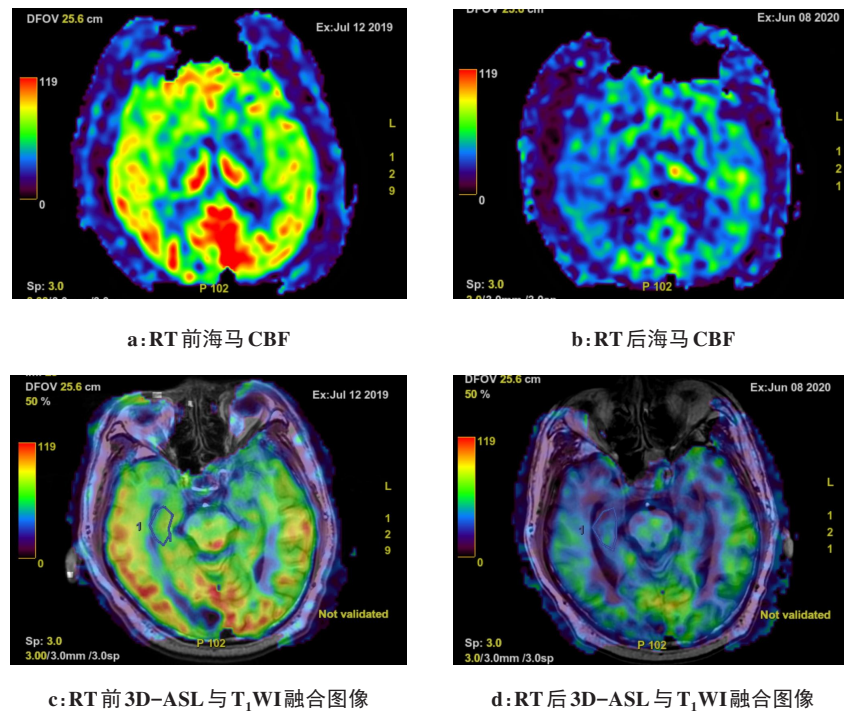


图3 长时间间隔RT前后海马CBF变化

Figure 3 Hippocampal CBF changes at long intervals before and after RT

### 3 讨论

本研究首先证实RT后海马CBF变化较体积更加显著,CBF变化应该作为海马RT反应的常规监测指标;其次,本研究发现入组患者海马CBF及体积变化有显著的剂量及时间依赖性。从BMs患者随访来看,随着接受WBRT的BMs患者生存时间延长,认知功能障碍的发生率也不断升高,主要表现为记忆障碍、失用、失语、失认等,严重影响患者的生活质量。认知功能障碍与海马损伤密切相关,其主要表现为海马体积减小与CBF的下降<sup>[12-13]</sup>。两次MR模拟定位扫描时间间隔对海马的CBF及体积具有显著影响。MR扫描时间间隔短时,本研究发现<1 Gy组、1~30 Gy组海马CBF与体积会出现短暂的升高,这些发现可能与海马区域的生理反应和病理变化有关。Chen等<sup>[14]</sup>发现RT后的一段时间内广义q-采样成像参数快速增加,这与海马的代谢及CBF的变化密切相关。射线的作用会导致血管的损伤,短时间内的修复反应引起海马CBF暂时性增加<sup>[15]</sup>。其次海马体积的变化差异不显著,这可能是与两次MR定位时间间隔短,海马体积变化尚未表现出来相关。

两次MR模拟定位扫描时间间隔长时,本研究观察到海马CBF与体积呈下降趋势。这可能与辐射对海马区域的直接和间接损伤有关。RT对人体组织造成的损伤并不是一过性,Eifel等<sup>[16]</sup>、Johansson等<sup>[17]</sup>报

道迟发性RT损伤甚至在治疗结束后几年才发生,而这主要表现在受照射部位纤维化、萎缩以及血管损伤。辐射会导致内皮细胞损伤,平滑肌细胞异常增殖、迁移及血小板聚集,血管壁增厚或形成微血栓,导致血管狭窄,可引起组织缺血、坏死,进而体积减小<sup>[18-20]</sup>。BMs患者WBRT后CBF与体积同步下降,但是下降幅度有显著差异。这是因为辐射诱导的海马缺血缺氧恶性循环首先会导致CBF的下降,进而引起体积的变化,海马萎缩具有显著滞后性。海马接受的剂量对CBF及体积的变化具有显著影响。本研究发现≤1 Gy组与1~30 Gy组差异性不显著,而其余组间海马CBF变化率差异显著,这可能是由于低中剂量组的海马CBF变化浮动较大。而在两次MR模拟定位扫描时间间隔<30 d时,<1 Gy组及1~30 Gy组海马CBF增加,≥30 Gy组的海马CBF下降。这种差异可能是由于高剂量辐射导致海马区域的血管损伤和血脑屏障破坏更加严重,进而影响海马CBF。

Song等<sup>[21]</sup>对小鼠FSaII纤维肉瘤肿瘤进行的研究表明,单次剂量20~30 Gy照射后1~5 d内,肿瘤血流灌注严重下降。高剂量的射线会导致血管在24 h内堵塞,进而导致血流在24 h内衰减40%,并持续72 h。Chen等<sup>[22]</sup>发现RT后脑区与海马功能连接的强度减低,且海马功能的表现与剂量有关,低剂量辐射损伤在1~3个月内引起短暂停神经损伤,但高剂量辐射会导致神经永久性损伤。这可能与本研究中海

马接受高剂量照射后血流出现显著下降现象相关。MR无创的灌注影像技术3D-ASL在肿瘤诊疗中应用日益广泛<sup>[23-24]</sup>。3D-ASL反映的CBF信息是追踪RT反应、预测放射性损伤及评价认知功能状态的重要生物学标记。Sun等<sup>[25]</sup>用3D-ASL测量皮层下血管性认知功能障碍(SVCI)患者的CBF变化,证明颞叶的CBF不足与SVCI严重程度有关。通过3D-ASL进行海马CBF的监测有利于及时对海马的放射性损伤进行临床干预,防止认知功能障碍的发生。

本研究的主要局限有以下几点:这是一项来自真实世界的回顾性探索性研究,时间跨度大,所有患者均在同一台设备、相同的扫描参数下获得影像;人组样本量较少,未能建立海马损伤可靠预测模型。本研究初步揭示WBRT后海马CBF、体积的变化规律,未来通过多中心的临床研究,构建WBRT后认知功能障碍发生的精确模型,为海马保护提供循证医学证据。综上所述,海马CBF与体积持续下降,并且有显著的时间剂量相关性,CBF下降较体积减小更加显著。海马CBF监测可以作为海马RT反应动态追踪可行方法及有效指标。

## 【参考文献】

- [1] Ernani V, Stinchcombe TE. Management of brain metastases in non-small-cell lung cancer[J]. J Oncol Pract, 2019, 15(11): 563-570.
- [2] Graus F, Walker RW, Allen JC. Brain metastases in children[J]. J Pediatr, 1983, 103(4): 558-561.
- [3] Kim JH, Jenrow KA, Brown SL. Mechanisms of radiation-induced normal tissue toxicity and implications for future clinical trials[J]. Radiat Oncol J, 2014, 32(3): 103-115.
- [4] Heo S, Prakash RS, Voss MW, et al. Resting hippocampal blood flow, spatial memory and aging[J]. Brain Res, 2010, 1315: 119-127.
- [5] 米小昆, 刘青蕊, 王佳, 等. 海马体积测量联合MMSE评分在认知障碍中的应用[J]. 实用放射学杂志, 2017, 33(2): 178-180.  
Mi XK, Liu QR, Wang J, et al. Hippocampal volume measurement with MMSE score in the application value of cognitive impairment[J]. Journal of Practical Radiology, 2017, 33(2): 178-180.
- [6] 徐亚利, 袁瑛, 陶晓峰. ASL在不同年龄段正常人脑血流量中的应用[J]. 实用放射学杂志, 2014(8): 1267-1270.  
Xu YL, Yuan Y, Tao XF. The application of ASL in assessing cerebral blood flow in healthy volunteers[J]. Journal of Practical Radiology, 2014(8): 1267-1270.
- [7] 沈艳勇, 赵鑫, 秦池, 等. 动脉自旋标记技术在孤独症谱系障碍伴或不伴全面发育迟缓中的应用[J]. 实用放射学杂志, 2024, 40(3): 443-446.  
Shen YY, Zhao X, Qin C, et al. Application of arterial spin labeling techniques in autism spectrum disorder with or without global developmental delay[J]. Journal of Practical Radiology, 2024, 40(3): 443-446.
- [8] 陈耿, 宣怡. 动脉自旋标记技术在颅脑疾病诊断中的临床应用[J]. 实用放射学杂志, 2008, 24(10): 1418-1420.  
Chen G, Huan Y. Clinical application of arterial spin labeling technique in diagnosis of craniocerebral diseases [J]. Journal of Practical Radiology, 2008, 24(10): 1418-1420.
- [9] 徐耀, 陈兰兰, 苏悦, 等. 轻度认知障碍及阿尔茨海默病患者脑血流灌注与认知功能的回归分析[J]. 中华医学杂志, 2019, 99(3): 193-197.  
Xu Y, Chen LL, Su Y, et al. Regression analysis of cerebral blood perfusion and cognitive function in patients with mild cognitive impairment and Alzheimer's disease[J]. National Medical Journal of China, 2019, 99(3): 193-197.
- [10] 曾善美, 刘恺, 张竟予, 等. 抑郁倾向Itpr2-/-小鼠海马3D-ASL灌注成像改变[J]. 南方医科大学学报, 2020, 40(1): 56-60.  
Zeng SM, Liu K, Zhang JY, et al. Changes in three-dimensional arterial spin labeling perfusion imaging of the hippocampus in depressive Itpr2-/-mice[J]. Journal of Southern Medical University, 2020, 40(1): 56-60.
- [11] Goda JS, Dutta D, Krishna U, et al. Hippocampal radiotherapy dose constraints for predicting long-term neurocognitive outcomes: mature data from a prospective trial in young patients with brain tumors[J]. Neuro Oncol, 2020, 22(11): 1677-1685.
- [12] Morley JE. An overview of cognitive impairment[J]. Clin Geriatr Med, 2018, 34(4): 505-513.
- [13] Li J, Cao D, Dimakopoulos V, et al. Anterior-posterior hippocampal dynamics support working memory processing[J]. J Neurosci, 2022, 42(3): 443-453.
- [14] Chen VC, Chuang W, Tsai YH, et al. Longitudinal assessment of chemotherapy-induced brain connectivity changes in cerebral white matter and its correlation with cognitive functioning using the GQI[J]. Front Neurol, 2024, 15: 1332984.
- [15] 李宁, 朱莹, 张文丽, 等. 氧化/抗氧化失衡与大鼠前脑缺血后海马CA1区神经元损伤的关系[J]. 第三军医大学学报, 2015, 37(24): 2411-2416.  
Li N, Zhu Y, Zhang WL, et al. Relationship of oxidation/antioxidation imbalance and hippocampal CA1 neuronal injury in rats at early stage of vascular dementia[J]. Journal of Third Military Medical University, 2015, 37(24): 2411-2416.
- [16] Eifel PJ, Donaldson SS, Thomas PR. Response of growing bone to irradiation: a proposed late effects scoring system[J]. Int J Radiat Oncol Biol Phys, 1995, 31(5): 1301-1307.
- [17] Johansson S, Svensson H, Denekamp J. Timescale of evolution of late radiation injury after postoperative radiotherapy of breast cancer patients[J]. Int J Radiat Oncol Biol Phys, 2000, 48(3): 745-750.
- [18] Popanda O, Marquardt JU, Chang-Claude J, et al. Genetic variation in normal tissue toxicity induced by ionizing radiation[J]. Mutat Res, 2009, 667(1/2): 58-69.
- [19] Fernet M, Hall J. Predictive markers for normal tissue reactions: fantasy or reality?[J]. Cancer Radiother, 2008, 12(6/7): 614-618.
- [20] Zhao W, Diz DI, Robbins ME. Oxidative damage pathways in relation to normal tissue injury[J]. Br J Radiol, 2007, 80(S1): S23-S31.
- [21] Song CW, Lee YJ, Griffin RJ, et al. Indirect tumor cell death after high-dose hypofractionated irradiation: implications for stereotactic body radiation therapy and stereotactic radiation surgery[J]. Int J Radiat Oncol Biol Phys, 2015, 93(1): 166-172.
- [22] Chen SC, Abe Y, Fang PT, et al. Prognosis of hippocampal function after sub-lethal irradiation brain injury in patients with nasopharyngeal carcinoma[J]. Sci Rep, 2017, 7(1): 14697.
- [23] Detre JA, Rao HY, Wang DJ, et al. Applications of arterial spin labeled MRI in the brain[J]. J Magn Reson Imaging, 2012, 35(5): 1026-1037.
- [24] McDonald RJ, McDonald JS, Kallmes DF, et al. Intracranial gadolinium deposition after contrast-enhanced MR imaging [J]. Radiology, 2015, 275(3): 772-782.
- [25] Sun YW, Cao WW, Ding WN, et al. Cerebral blood flow alterations as assessed by 3D ASL in cognitive impairment in patients with subcortical vascular cognitive impairment: a marker for disease severity[J]. Front Aging Neurosci, 2016, 8: 211.

(编辑:陈丽霞)